Available online at www.sciencedirect.com
SCIENCE DIRECT®
Journal of Sound and Vibration 288 (2005) 1011–1025
JOURNAL OF SOUND AND VIBRATION
www.elsevier.com/locate/jsvi

Time domain responses of a prestressed beam and prestress identification

S.S. Law*, Z.R. Lu

Civil and Structural Engineering Department, The Hong Kong Polytechnic University, Hunghom, Kowloon, Hong Kong

Received 22 December 2003; received in revised form 14 June 2004; accepted 15 January 2005
Available online 17 May 2005

Abstract

The time-domain response of a prestressed Euler–Bernoulli beam under external excitation is studied based on modal superposition. The prestress force is then identified in the time domain by a system identification approach and Tikhonov regularization technique is used to provide bounds to the ill-conditioned results in the identified problem. Both measured displacements and strains are used. The noise effect is improved using the orthogonal polynomial function, and cases with either sinusoidal or impulsive excitations are illustrated to give very good results from the lower three measured modes and data obtained from three measurement points. Work in this paper demonstrates the feasibility of indirectly identifying the prestress force in a beam.

1. Introduction

Many developed countries are facing the problem of aging infrastructure and a limited budget on their maintenance. A quick and non-destructive test method to assess the condition of existing structures is required for their maintenance and repair. Many of the physical parameters of the structure, such as the Young's modulus and the second moment of area of the cross-section, are candidates in the set of variable to define the condition of the structure. Prestressing force has

*Corresponding author. Tel.: +852 2766 6062; fax: +852 2334 6389.
E-mail address: cesslaw@polyu.edu.hk (S.S. Law).

0022-460X/$ - see front matter © 2005 Elsevier Ltd. All rights reserved.
doi:10.1016/j.jsv.2005.01.045

Nomenclature

ρ	mass density of the beam material
A	cross-sectional area
h_0	the height of the beam
b	the width of the beam
c	the viscous damping of the beam
$P(t)$	the external exciting force
E	Young's modulus
$[I]$	unity matrix
I_0	the second moment of area of the beam cross-section
T	prestress force
$y(x,t)$	transverse displacement of the beam
$Y_i(x)$	the ith mode shape of the beam
$q_i(t)$	modal coordinate
$[M]$	modal mass matrix
$[C]$	modal damping matrix
$[K]$	modal stiffness matrix
$[K']$	modal stiffness reduction due to the prestress force
N	number of modes used
N_f	number of the polynomial terms used
λ	regularization parameter

been used widely with long span structure, and it is the most important factor to describe the load-carrying capacity of the structure.

This paper addresses the problem of prestress force identification in a bridge deck modeled as a simply supported beam. The bridge deck may lose some of its prestress force due to creep and relaxation from long period of service under design or overloaded vehicles. A large reduction of the prestress force from the design value could lead to serviceability and safety problems. Therefore assessment on the magnitude of the prestress force or the loss of prestress force in the bridge deck is important for its load-carrying capacity assessment. However existing prestress force cannot be estimated directly unless the bridge deck has been instrumented at the time of construction. Several researchers [1] tried to predict the loss of prestress based on a damage index derived from the derivatives of mode shapes without success. Others [2] studied the behaviour of a beam with unbonded tendons, and a formula was proposed for the prediction of the modal frequency for a given prestress force with laboratory and field test verifications. Saiidi et al. [3] reported a study with modal frequency due to the prestress force with laboratory test results.

No work has been reported on the effect of prestress on the dynamic responses of a beam and on any successful method to identify directly or indirectly the prestress force of a beam. Saiidi et al. [3] showed that the sensitivity of the modal frequency to prestress decreases with higher vibration modes, and the prestress force affects the first few lower modes more significantly than the higher ones. Consequently the prestress force would be difficult to identify from the modal frequencies. Also Abraham et al. [1] reported that the mode shapes remain almost identical with different prestress force in the beam, and it will also be difficult to identify the force from the measured mode shapes.

The dynamic response of a prestress beam is studied in this paper based on modal superposition, and the contribution from the higher modes is found less than that from lower modes as with a non-prestressed beam. An inverse problem to identify the prestress force is then formulated taking only the prestress force and both the prestress force and the flexural rigidity of the beam as variables in the identification with external excitation. The damped least-squares method with regularisation is used for the solution. Orthogonal polynomial function is used to approximate the measured strain responses to remove the measurement noise effect, and the effectiveness of using an impulsive force in the identification is also illustrated. The work

presented in this paper indicates that the identification of prestress force with normal modal testing technique is feasible even with noisy data.

2. Forward problem

2.1. Equation of motion

The bridge deck is modeled as a single-span simply supported prestressed uniform Euler–Bernoulli beam subjected to an external excitation force $P(t)$ acting at a distance x_p from the left support as shown in Fig. 1. The equation of motion of the beam can be written as

$$\rho A \frac{\partial^2 y(x,t)}{\partial t^2} + c \frac{\partial y(x,t)}{\partial t} + T \frac{\partial^2 y(x,t)}{\partial x^2} + \frac{\partial^2}{\partial x^2} EI_0 \frac{\partial^2 y(x,t)}{\partial x^2} = P(t)\delta(x - x_p), \tag{1}$$

where ρ is the mass density of the beam, A is the cross-sectional area, c is the damping of the beam, E is the Young's modulus of material, $I_0 = bh_0^3/12$ is the moment of inertia of the beam cross-section, b is the width of the beam, h_0 is the height of the beam, T is the externally applied compressive axial force (note that compressive is positive and tension is negative), $y(x,t)$ is the transverse displacement function of the beam, and $\delta(x)$ is the Dirac delta function.

The prestress is assumed unbonded with the concrete, and it is constant along the whole beam. The tendon eccentricity gives rise to a static moment effect on the beam section, and it has not any relationship with its dynamic properties. It is therefore not represented in Eq. (1).

2.2. Modal responses

On the basis of modal superposition, the dynamic deflection $y(x,t)$ of the beam can be expressed as

$$y(x,t) = \sum_{i=1}^{\infty} Y_i(x) q_i(t), \tag{2}$$

where $Y_i(x)$ is the mode shape function of the ith mode and $q_i(t)$ is the ith modal amplitude.

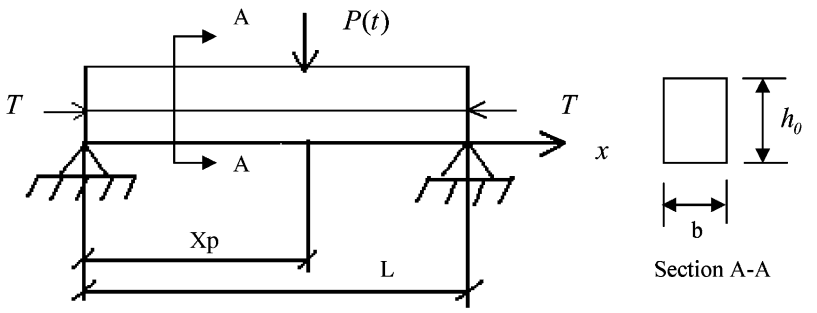

Fig. 1. Prestressed beam model.

Substituting Eq. (2) into Eq. (1), multiplying each term by $Y_j(x)$, integrating with respect to x between 0 and L and applying the modal orthogonality conditions, we have

$$\ddot{q}_i(t) + 2\xi_i\bar{\omega}_i\dot{q}(t) + \bar{\omega}_i^2 q_i(t) = \frac{1}{m_i} f_i(t), \tag{3}$$

where $\bar{\omega}_i = \sqrt{(EI_0/(\rho A)(\mathrm{i}\pi/L)^4 - T/(\rho A)(\mathrm{i}\pi/L)^2)}$, ξ_i and m_i are the reduced modal frequency, the damping ratio and the modal mass of the ith mode; $f_i(t) = P(t)\,Y_i(x_p)$ is the modal force. The modal shape functions of the prestressed beam resemble those of a beam without prestress force [1] and it is written in the normalized form as $Y_i(x) = \sqrt{2/(\rho AL)}\sin(\mathrm{i}\pi/L)x$ for a simply supported beam, and

$$m_i = \int_0^L \rho A\, Y_i^2(x)\,\mathrm{d}x = 1. \tag{4}$$

Writing Eq. (3) in matrix form

$$[I]\{\ddot{Q}(t)\} + [C]\{\dot{Q}(t)\} + ([K] - [K'])\{Q(t)\} = \{F(t)\}, \tag{5}$$

where

$$[C] = \mathrm{diag}(2\xi_i\omega_i), \quad [K] = \mathrm{diag}\left(\frac{EI_0}{\rho A}\left(\frac{\mathrm{i}\pi}{L}\right)^4\right), \quad [K'] = \mathrm{diag}\left(\frac{T}{\rho A}\left(\frac{\mathrm{i}\pi}{L}\right)^2\right),$$

$$\{Q(t)\} = \{q_1(t), q_2(t), \ldots, q_n(t)\}^{\mathrm{T}}, \quad \{F(t)\} = \{f_1(t), f_2(t), \ldots, f_n(t)\}^{\mathrm{T}}$$

and $[I]$ is the unity matrix.

We can determine $\bar{\omega}_i$ for $T \leqslant T_{\mathrm{cr}}$ where $T_{\mathrm{cr}} = \pi^2 EI_0/L^2$ is the critical buckling load of the beam. The modal response is computed in the time domain numerically using the Newmark's integration scheme [4].

3. Inverse problem

3.1. Prestress force identification from measured displacements

Expressing the measured displacements $y(x_m, t)$ at a point x_m from the left support in modal coordinates

$$y(x_m, t) = \sum_{i=1}^{N} Y_i(x) q_i(t), \quad (m = 1, 2, \ldots, N_m) \tag{6a}$$

or in matrix form as

$$\{y\}_{N_m\times 1} = [Y]_{N_m\times N}\{q\}_{N\times 1}, \tag{6b}$$

where $\{y\}_{N_m\times 1}$ is the vector of displacements at N_m measurement locations, and N is the number of measured modes in the responses. The vector of generalized coordinates can be written using

the least-squares pseudo-inverse

$$\{q\}_{N\times 1} = ([Y]^{\mathrm{T}}_{N\times N_m}[Y]_{N_m\times N})^{-1}[Y]^{\mathrm{T}}_{N\times N_m}\{y\}_{N_m\times 1}. \tag{7}$$

The modal velocity and acceleration of the beam responses can be obtained from Eq. (7) by numerical methods. However, when the measurements are polluted by noise, the use of central difference method to calculate the modal velocity and acceleration will lead to large computation error. Therefore the generalized orthogonal polynomial [5] is used to model the measured displacement as

$$y(x_j, t) = \sum_{i}^{N_f} a_i G_i(t), \tag{8}$$

where $y(x_j, t)$ is the approximated displacement at the jth measuring point. N_f is the order of the orthogonal polynomial function. The velocity and acceleration are then approximated by the first and second derivatives of the orthogonal polynomial. It is to note that the order of the orthogonal polynomial function N_f has large effects on the accuracy of velocity and acceleration approximated by the first and second derivatives of the orthogonal polynomial. Study in the present paper found that $N_f = 20$ is the optimal order such that the velocity and acceleration can be obtained accurately.

Substituting Eq. (8) into Eq. (6) and writing in matrix form, we have,

$$\begin{aligned}
\{y\}_{N_m\times 1} &= [A]_{N_m\times N_f}[G]_{N_f\times 1},\\
\{\dot{y}\}_{N_m\times 1} &= [A]_{N_m\times N_f}[\dot{G}]_{N_f\times 1},\\
\{\ddot{y}\}_{N_m\times 1} &= [A]_{N_m\times N_f}[\ddot{G}]_{N_f\times 1},
\end{aligned} \tag{9}$$

where $[A]_{N_m\times N_f}$, $[G]_{N_f\times 1}$, $[\dot{G}]_{N_f\times 1}$, $[\ddot{G}]_{N_f\times 1}$ are the coefficient matrix of the polynomial, the orthogonal polynomial matrix, the first and second derivatives of the orthogonal polynomial variable matrix, respectively. The coefficient matrix $[A]$ can be obtained by the least-squares method from Eq. (9)

$$[A]_{N_m\times N_f} = \{y\}_{N_m\times 1}[G]^{\mathrm{T}}_{1\times N_f}([G]_{N_f\times 1}[G]^{\mathrm{T}}_{1\times N_f})^{-1}. \tag{10}$$

Substituting matrix $[A]$ into Eq. (9), we can get $\{\dot{y}\}$ and $\{\ddot{y}\}$. And substituting $\{y\}, \{\dot{y}\}, \{\ddot{y}\}$ and the derivatives of $[G]$ into Eq. (7), we can obtain the modal displacement q, modal velocity $\dot{q}$ and modal acceleration $\ddot{q}$. Substituting further q, $\dot{q}$ and $\ddot{q}$ into Eq. (5), and after transformation, we have

$$[K']\{Q(t)\} = [I]\{\ddot{Q}(t)\} + [C]\{\dot{Q}(t)\} + [K]\{Q(t)\} - \{F(t)\}. \tag{11}$$

Matrix $[K']$ contains the prestress force T which is assumed constant throughout the length of the beam. Matrix $[C]$ contains the modal damping ξ_i and modal frequency ω_i which are assumed unchanged, and matrix $[K]$ contains the system parameters of the beam which are also assumed unchanged. The inverse problem is to solve Eq. (11) in time domain to get the prestress force T. Rewriting Eq. (11)

$$\{B\}_{n\times 1}T = \{\bar{F}\}_{n\times 1}, \tag{12}$$

where

$$\{B\} = \begin{bmatrix} \left(\frac{\pi}{L}\right)^2 \frac{1}{\rho A} & 0 & 0 & 0 \\ 0 & \left(\frac{2\pi}{L}\right)^2 \frac{1}{\rho A} & 0 & 0 \\ 0 & 0 & \ddots & 0 \\ 0 & 0 & 0 & \left(\frac{n\pi}{L}\right)^2 \frac{1}{\rho A} \end{bmatrix}_{n\times n} \begin{Bmatrix} q_1(t) \\ q_2(t) \\ \vdots \\ q_n(t) \end{Bmatrix}_{n\times 1}$$

and vector $[\bar{F}]$ contains all the terms on the right-hand side of Eq. (11). From Eq. (12) one can see, the equation number is n but the unknown is only one, T, so the prestress force T can be calculated directly by the simple least-squares method

$$T = (\{B\}^{\mathrm{T}}\{B\})^{-1}\{B\}^{\mathrm{T}}\{\bar{F}\}. \tag{13}$$

In order to have bounds on the ill-conditioned solution, the damped least-squares method (DLS) is used and singular value decomposition is used in the pseudo-inverse computation. Eq. (13) is written in the following form using the DLS method:

$$T = (\{B\}^{\mathrm{T}}\{B\} + \lambda I)^{-1}\{B\}^{\mathrm{T}}\{\bar{F}\}, \tag{14}$$

where λ is the non-negative damping coefficient governing the contribution of the least-squares error in the solution. The solution of Eq. (14) is equivalent to minimizing the function

$$J(T, \lambda) = \min(\|\{B\}T - \{\bar{F}\}\|^2 + \lambda\|T\|^2) \tag{15}$$

with the second term in Eq. (15) providing bounds to the solution.

3.2. Identification from measured strains

The strain at the bottom of the beam at a point x_m from the left support can be expressed similar to Eq. (6) in terms of the generalized coordinates as

$$\varepsilon(x_m, t) = -\frac{h_0}{2}\sum_{i=1}^{N} Y''(x_m)q_i(t) \quad (m = 1, 2, \ldots, N_m), \tag{16}$$

where h_0 is the depth of the beam. Eq. (16) can be written as

$$\{\varepsilon\}_{N_m\times 1} = [Y'']_{N_m\times N}\{q\}_{N\times 1}, \tag{17}$$

where $\{\varepsilon\}_{N_m\times 1}$ is the vector of strains at N_m measurement locations. Again the strain at the jth measuring point can be approximated by the orthogonal function $G(t)$ as

$$\varepsilon(x_j, t) = \sum_{i}^{N_f} a_i G_i(t). \tag{18}$$

The rest of the computation in the identification is similar to that for identification from measured displacements mentioned above.

3.3. Identification of both prestress force and the flexural rigidity of the beam

Other variables in the system should also be included in the identification for a real application. Since the dimensions of the beam can be measured accurately, and the modal damping can be estimated from a preliminary spectral analysis before the identification, the only variable with uncertainty is the flexural rigidity EI_0 of the beam section. If we have a uniform uncracked beam, we have both T and EI_0 as the two variables in the identification. Rewriting Eq. (11) as

$$\begin{aligned}
&\left(T \begin{bmatrix} \left(\frac{\pi}{L}\right)^2 \frac{1}{\rho A} & 0 & 0 & 0 \\ 0 & \left(\frac{2\pi}{L}\right)^2 \frac{1}{\rho A} & 0 & 0 \\ 0 & 0 & \ddots & 0 \\ 0 & 0 & 0 & \left(\frac{n\pi}{L}\right)^2 \frac{1}{\rho A} \end{bmatrix}_{n\times n} \right. \\
&\left. -EI_0 \begin{bmatrix} \left(\frac{\pi}{L}\right)^4 \frac{1}{\rho A} & 0 & 0 & 0 \\ 0 & \left(\frac{2\pi}{L}\right)^4 \frac{1}{\rho A} & 0 & 0 \\ 0 & 0 & \ddots & 0 \\ 0 & 0 & 0 & \left(\frac{n\pi}{L}\right)^4 \frac{1}{\rho A} \end{bmatrix}_{n\times n} \right) \begin{Bmatrix} q_1(t) \\ q_2(t) \\ \vdots \\ q_n(t) \end{Bmatrix} \\
&= \begin{bmatrix} 1 & 0 & 0 & 0 \\ 0 & 1 & 0 & 0 \\ 0 & 0 & \ddots & 0 \\ 0 & 0 & 0 & 1 \end{bmatrix}_{n\times n} \begin{Bmatrix} \ddot{q}_1(t) \\ \ddot{q}_2(t) \\ \vdots \\ \ddot{q}_n(t) \end{Bmatrix}_{n\times 1} + \begin{bmatrix} 2\xi_1\omega_1 & 0 & 0 & 0 \\ 0 & 2\xi_2\omega_2 & 0 & 0 \\ 0 & 0 & \ddots & 0 \\ 0 & 0 & 0 & 2\xi_n\omega_n \end{bmatrix}_{n\times n} \begin{Bmatrix} \dot{q}_1(t) \\ \dot{q}_2(t) \\ \vdots \\ \dot{q}_n(t) \end{Bmatrix}_{n\times 1} \\
&\quad - \begin{Bmatrix} f_1(t) \\ f_2(t) \\ \vdots \\ f_n(t) \end{Bmatrix}_{n\times 1} .
\end{aligned} \tag{19}$$

The inverse problem is to solve Eq. (19) in time domain at each time step to get the prestress force T and the flexural rigidity EI_0. Rewriting Eq. (19) in a simple form

$$[B]\{X\} = \{\bar{F}\}_{n\times 1}, \tag{20}$$

where

$$[B] = \begin{bmatrix} B_T & 0 \\ 0 & B_{EI} \end{bmatrix}, \quad \{X\} = \begin{Bmatrix} T \\ EI_0 \end{Bmatrix},$$

$$\{B_T\} = \begin{bmatrix} \left(\frac{\pi}{L}\right)^2 \frac{1}{\rho A} & 0 & 0 & 0 \\ 0 & \left(\frac{2\pi}{L}\right)^2 \frac{1}{\rho A} & 0 & 0 \\ 0 & 0 & \ddots & 0 \\ 0 & 0 & 0 & \left(\frac{n\pi}{L}\right)^2 \frac{1}{\rho A} \end{bmatrix}_{n\times n} \begin{Bmatrix} q_1(t) \\ q_2(t) \\ \vdots \\ q_n(t) \end{Bmatrix}_{n\times 1},$$

$$\{B_{EI}\} = \begin{bmatrix} \left(\frac{\pi}{L}\right)^4 \frac{1}{\rho A} & 0 & 0 & 0 \\ 0 & \left(\frac{2\pi}{L}\right)^4 \frac{1}{\rho A} & 0 & 0 \\ 0 & 0 & \ddots & 0 \\ 0 & 0 & 0 & \left(\frac{n\pi}{L}\right)^4 \frac{1}{\rho A} \end{bmatrix}_{n\times n} \begin{Bmatrix} q_1(t) \\ q_2(t) \\ \vdots \\ q_n(t) \end{Bmatrix}_{n\times 1}.$$

Again the prestress force T and the flexural rigidity EI_0 can be calculated directly by the simple least-squares method

$$\{X\} = ([B]^{\mathrm{T}}[B])^{-1}[B]^{\mathrm{T}}\{\bar{F}\} \tag{21}$$

or in the following form using the DLS method.

$$\{X\} = ([B]^{\mathrm{T}}[B] + \lambda[I])^{-1}[B]^{\mathrm{T}}\{\bar{F}\}. \tag{22}$$

Both the prestress force and the flexural rigidity of the beam are identified at each time step. The dimension of the variable $\{X\}$ is $2n_t \times 1$, where n_t is the total time steps. The variable vector $[X]$ is defined with these two variables appearing in alternative order, i.e. the prestress force takes up the odd terms of the vector $[X]$ while the flexural rigidity takes up the even terms.

4. Simulation and results

4.1. The prestress beam

A 30 m long simply supported Euler–Bernoulli beam with an axial prestress force of $0.3T_{\mathrm{cr}} = 8.2247 \times 10^6$ N is studied. The first six natural frequencies of the beam are: 1.03, 4.75, 10.11, 19.56, 30.67 and 44.25 Hz. The damping ratios for these six modes are all equal to 0.02. The prestress

force is constant along the beam. The external exciting force is

$$f(t) = 12000[1 + 0.1\sin(10\pi t) + 0.05\sin(40\pi t)]\,\mathrm{N}$$

and it is applied at 7 m from the left support to excite the lower modes. The parameters of the beam are: $\rho A = 5.0 \times 10^3\,\mathrm{kg/m}$, $E = 5 \times 10^{10}\,\mathrm{N/m^2}$, $L = 30\,\mathrm{m}$, $b = 0.6\,\mathrm{m}$, and $h_0 = 1.0\,\mathrm{m}$. The flexural rigidity EI_0 of the beam is calculated as $2.5 \times 10^9\,\mathrm{N\,m^2}$.

4.2. Effect of prestress on the modal frequency and responses

Table 1 shows the modal frequencies of the first five modes of the above beam when $T = 0.1T_{cr}$, $T = 0.3T_{cr}$ and $T = 0.5T_{cr}$, respectively, and the lower modal frequencies are seen more affected by the axial compression than the higher modes. The frequency of the beam decreases with an increase in the axial compression and vice versa. This is due to the "compression softening" effect [6] from the prestress force.

Figs. 2 and 3 show the effect of the prestress force on the responses of the beam when $T = 0.1T_{cr}$ and $T = 0.3T_{cr}$, respectively when only three modes are included. It is seen that the effect of prestress is most significant with the displacement responses and the acceleration responses are least affected, and such effect increases with larger prestress in the beam.

4.3. Prestress force identification

White noise is added to the calculated displacements and strains to simulate the polluted measurements as follows:

$$y = y_{\mathrm{calculated}} + Ep\,N_{\mathrm{oise}}\,\mathrm{var}(y_{\mathrm{calculated}}),$$
$$\varepsilon = \varepsilon_{\mathrm{calculated}} + Ep\,N_{\mathrm{oise}}\,\mathrm{var}(\varepsilon_{\mathrm{calculated}}),$$

where y and ε are the vectors of polluted displacements and strains respectively, Ep is the noise level, N_{oise} is a standard normal distribution vector with zero mean and unit standard deviation, var(•) is the variance of the time history, $y_{\mathrm{calculated}}$ and $\varepsilon_{\mathrm{calculated}}$ are the vectors of calculated displacements and strains. Five percent and 10% noise levels are included in the study in this paper.

The above beam with $T = 0.3T_{cr}$ axial force is studied. The first three modes are used in the calculation. Measured displacements at $\frac{1}{4}L, \frac{1}{2}L$ and $\frac{3}{4}L$ are used in the identification. The sampling

Table 1
Modal frequencies corresponding to different prestress force

Prestress force	Frequency (Hz)				
	1st	2nd	3rd	4th	5th
$T = 0$	1.23	4.94	11.11	19.75	30.86
$T = 0.1T_{cr}$	1.17	4.88	11.05	19.69	30.80
$T = 0.3T_{cr}$	1.03	4.75	10.92	19.56	30.67
$T = 0.5T_{cr}$	0.87	4.62	10.80	19.44	30.55

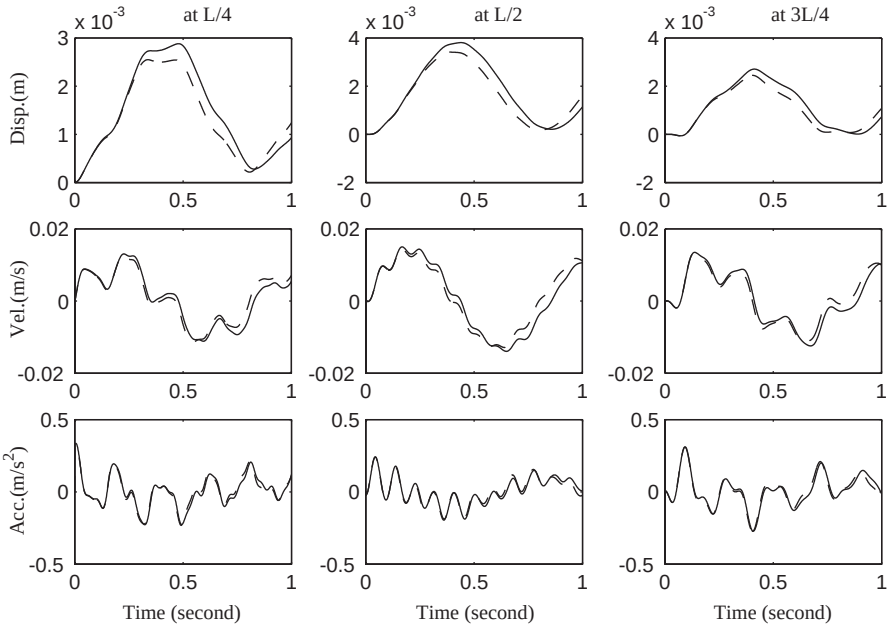

Fig. 2. Difference in responses ($T = 0.1\,T_{cr}$) (—, with prestress force; ---, without prestress force).

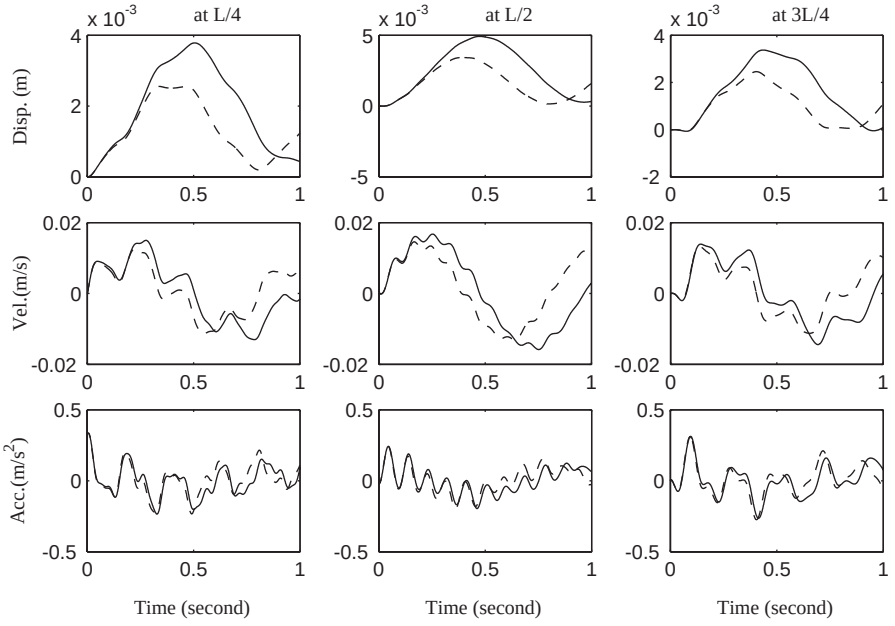

Fig. 3. Difference in responses ($T = 0.3\,T_{cr}$) (—, with prestress force; ---, without prestress force).

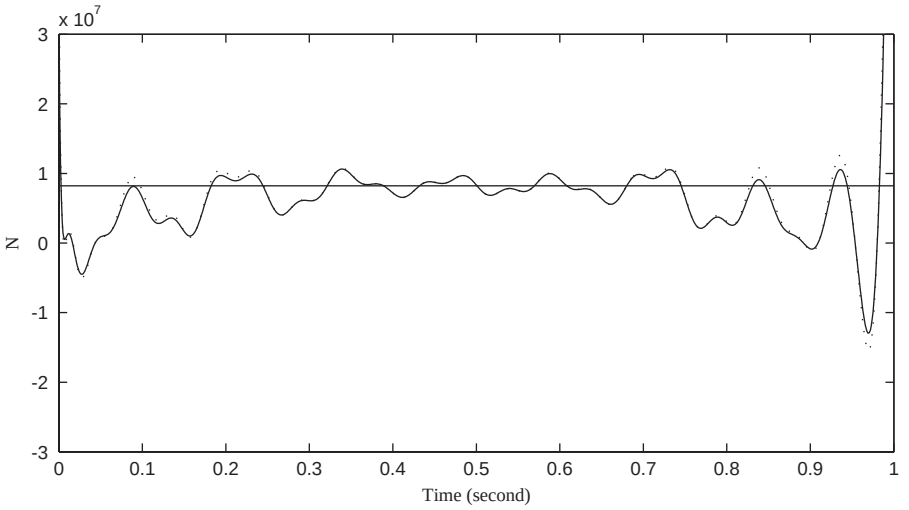

Fig. 4. Prestress force identification from three modes (—, true; ----, identified 5% noise; ..., identified 10% noise).

frequency is 1000 Hz, which is larger than 20 times the highest frequency of interest at 44.25 Hz. The beam is assumed at rest initially.

Fig. 4 shows the identified results from measured strains with 5% and 10% noise with the corresponding optimal regularization parameter equals to 3.4×10^{-6} and 6.1×10^{-6}, respectively. There is only a slight difference in the time histories of the identified prestress from both cases. This is because the measurements have been approximated with 20 terms of the orthogonal functions and the velocities and accelerations are subsequently obtained by directly differentiating the functions. This shows that the orthogonal function approach is effective in eliminating the noise in the measured data.

Large responses are found close to the start and end of the time histories while those in the middle halve vary closely around the true value. This is because the response is a discontinuous function of time at these two time instances. The second term in Eq. (22) provides bounds to the solution. When the regularization parameter λ approaches zero, the estimated vector $\{\bar{F}\}$ approaches the solution obtained from the least-squares method. In practice, the expected value of λ is not known, and the error between the true and the estimated forces is minimized [7] for a specific range of λ.

4.4. Identification using impulsive excitation

An impulsive force is also used to identify the prestress force, which acts on the beam between $t = 0.05$ s to 0.15 s. The magnitude of the force is 9500 N simulating the impact excitation produced by a 125 kg weight free falling for 1 m on the beam. The weight is assumed bounced off the beam after impact, and the effect of the falling mass after the impact is ignored. The force is applied at 7 m from the left support and it can be expressed in the following form:

$$f(t) = \begin{cases} 190000(t - 0.05)N & (0.05 \leqslant t \leqslant 0.1), \\ 190000(0.15 - t)N & (0.1 \leqslant t \leqslant 0.15). \end{cases}$$

A Fourier series is used to model the force as

$$f(t) = \alpha_0 + \sum_{k=1}^{\infty} \alpha_k \cos \frac{2k\pi t}{T} + \sum_{k=1}^{\infty} \beta_k \sin \frac{2k\pi t}{T},$$

where

$$\alpha_0 = \frac{1}{T}\int_0^T f(t)\,\mathrm{d}t,$$

$$\alpha_k = \frac{2}{T}\int_0^T f(t)\cos\frac{2k\pi t}{T}\,\mathrm{d}t \quad \text{and} \quad \beta_k = \frac{2}{T}\int_0^T f(t)\sin\frac{2k\pi t}{T}\,\mathrm{d}t.$$

Forty terms in the series are used to include the higher frequencies with the impulsive force. The sampling frequency is 1000 Hz, and the first three modes and three displacement measurements evenly distributed along the beam are used in the identification. Five percent noise is included in the identification. Fig. 5 shows that the identified prestress force obtained from using an optimal regularization parameter of 4.1×10^{-6} and it is found fluctuating closely around the true value.

4.5. Identification of both prestress force and the flexural rigidity of the beam

The same system as for the last study is used here, and the flexural rigidity EI_0 of the beam is $2.5 \times 10^9\,\mathrm{N\,m^2}$. The sampling frequency is 1000 Hz, and the first three modes and three evenly distributed displacement measurements are used in the identification. Also 5% noise is included in the identification. All other parameters remain unchanged.

Fig. 6 shows that both the identified prestress force and the flexural stiffness are fluctuating around the true values. The corresponding optimal regularization parameter is 2.7×10^{-6}. This shows further the effectiveness of the proposed method with multiple parameters identification.

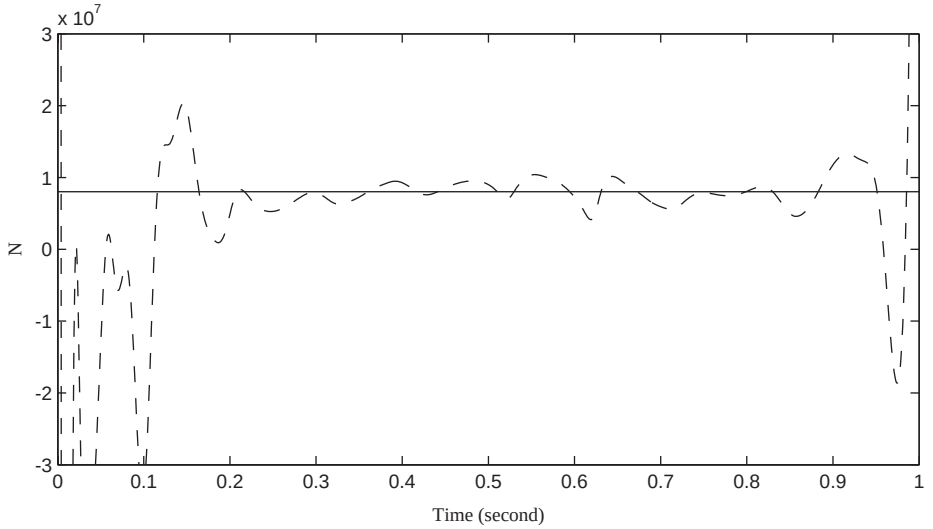

Fig. 5. Prestress force identified from impulsive force (—, true; ----, identified).

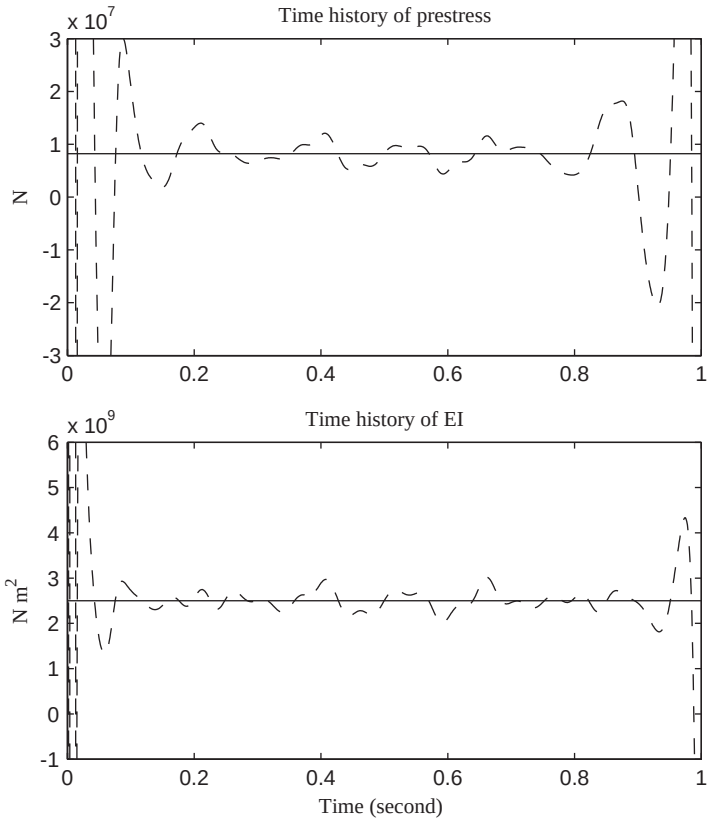

Fig. 6. Identification of prestress force and flexural rigidity (—, true; ----, identified).

4.6. Sensitivity of the proposed method to prestress force magnitude

In most cases of construction with prestress, the prestress force in a beam component is relatively small. A study is therefore made to study the errors involved in the identification of different magnitude of prestress force with different noise levels. The same beam and excitation for the last study is used. Five prestress levels and three noise levels are studied and the summation of error of the identified force according to Eq. (23) is shown in Table 2. The time histories of the identified prestress force which are $0.01T_{cr}$, $0.1T_{cr}$ and $0.3T_{cr}$ under 10% noise level are shown in Fig. 7 obtained from using an optimal regularization parameter of 6.1×10^{-6}.

$$\text{error} = \frac{\|T_{\text{pid}} - T_{\text{ptrue}}\|}{\|T_{\text{ptrue}}\|} \times 100\%. \tag{23}$$

The noise level is not important to the identification except for the case of a small prestress force of $0.01T_{cr}$. However detail inspection of Fig. 7 shows that all the curves are fluctuating around their corresponding true values. The sum of squares error or the variance of the identified forces is of the same order for all the cases studied indicating same order of accuracy in all the identifications. This also shows that the proposed method is insensitive to the level of prestress force. The large percentage

Table 2
Error percentage (%) and sum of squares error in the identified prestress force for different noise level

Prestress force	1% noise	5% noise	10% noise
$0.01T_{cr}$	$173/(7.77 \times 10^7)$	$218.3/(1.1 \times 10^8)$	$237.88/(1.37 \times 10^8)$
$0.05T_{cr}$	$75.53/(1.79 \times 10^8)$	$81.46/(2.16 \times 10^8)$	$86.46((2.53 \times 10^8))$
$0.1T_{cr}$	$46.37/(2.19 \times 10^8)$	$48.33/(2.48 \times 10^8)$	$50.29/(2.8 \times 10^8)$
$0.3T_{cr}$	$31.02(3.03 \times 10^8)$	$31.86(3.30 \times 10^8)$	$32.8(3.66 \times 10^8)$
$0.5T_{cr}$	$21.6/(3.43 \times 10^8)$	$21.62/(3.48 \times 10^8)$	$22.91/(3.56 \times 10^8)$

Note: (•) denotes the sum of squares error.

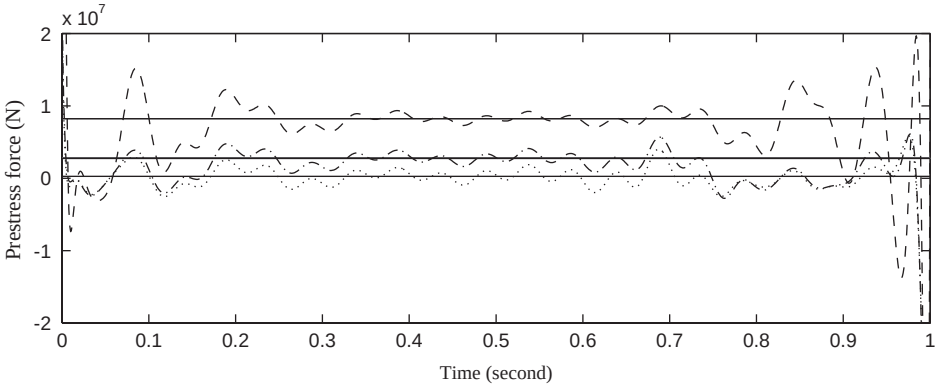

Fig. 7. Identification of different magnitude of prestress force (—, true; ----, $T = 0.3\,T_{cr}$; –.–.–., $T = 0.1\,T_{cr}$; …, $T = 0.01\,T_{cr}$).

error for a small prestress force arises from a small denominator as calculated from Eq. (23). Furthermore, over 90% of the force time history in the middle give close to true values of the force with smaller fluctuations indicating the good accuracy of the proposed method.

5. Conclusion

A new method to identify the prestress force in a prestressed concrete beam is proposed. The prestress force in a beam has been identified accurately with or without the flexural rigidity of the beam in the identification. The noise effect is improved using the orthogonal polynomial function. Both the sinusoidal and impulsive excitation could give good results from the lower three measured modes and strain or displacement obtained from only three measuring points. This work indicates that indirect measurement of the prestress force in a beam is feasible.

Acknowledgements

The work described in this paper was supported by a research grant from the Hong Kong Polytechnic University.

References

[1] M.A. Abraham, S.Y. Park, N. Stubbs, Loss of prestress prediction on nondestructive damage location algorithms, *SPIE, Smart Structures and Materials* 2446 (1995) 60–67.
[2] A. Miyamoto, K. Tei, H. Nakamura, J.W. Bull, Behavior of prestressed beam strengthened with external tendons, *Journal of Structural Engineering* 126 (9) (2000) 1033–1044.
[3] N. Saiidi, B. Douglas, S. Feng, Prestress force effect on vibration frequency of concrete bridges, *Journal of Structural Engineering* 120 (7) (1994) 2233–2241.
[4] N.W. Newmark, A method of computation for structural dynamics, *Journal of Engineering Mechanics Division, ASCE* 85 (3) (1959) 67–94.
[5] S.S. Law, X.Q. Zhu, Study on different beam models in moving force identification, *Journal of Sound and Vibration* 234 (2000) 661–679.
[6] F.S. Tse, I.E. Morse, R.T. Hinkle, *Mechanical Vibrations, Theory and Applications*, Allyn and Bacon, Boston, MA, 1978.
[7] J.C. Santantamarina, D. Fratta, *Introduction to Discrete Signals and Inverse Problems in Civil Engineering*, ASCE Press, New York, 1998, pp. 200–238.